



## Ocean-atmosphere interactions: Different organic components across Pacific and Southern Oceans



Jiyi Jang<sup>a</sup>, Jiyeon Park<sup>a,\*</sup>, Jongkwan Park<sup>b</sup>, Young Jun Yoon<sup>a</sup>, Manuel Dall'Osto<sup>c</sup>, Ki-Tae Park<sup>a</sup>, Eunho Jang<sup>a,d</sup>, Ji Yi Lee<sup>e</sup>, Kyung Hwa Cho<sup>f</sup>, Bang Yong Lee<sup>a</sup>

<sup>a</sup> Korea Polar Research Institute, 26, Songdomirae-ro, Yeosu-gu, Incheon 21990, Republic of Korea

<sup>b</sup> Department of Environment & Energy Engineering, Changwon National University, 20 Changwondaehak-ro, Changwon-si, Gyeongsangnam-do 51140, Republic of Korea

<sup>c</sup> Institut de Ciències del Mar, CSIC, Pg. Marítim de la Barceloneta 37-49, Barcelona, Catalonia 08003, Spain

<sup>d</sup> University of Science and Technology, 217, Gajeong-ro, Yuseong-gu, Daejeon 34113, Republic of Korea

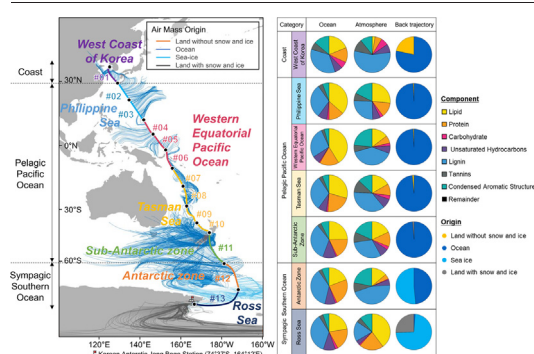
<sup>e</sup> Department of Environmental Science and Engineering, Ewha Womans University, Seoul 03760, Republic of Korea

<sup>f</sup> Ulsan National Institute of Science and Technology, 50, UNIST-gil, Eonyang-eup, Ulsan-gun, Ulsan 44919, Republic of Korea

### HIGHLIGHTS

- Seawater and aerosol chemical composition in Pacific and Southern Oceans
- Lignin-like and lipid-like OM were dominant in seawater.
- Lipid-like OM was enriched in ocean and aerosol due to the presence of sea ice.
- Oceans have different sources affecting ocean-atmosphere interactions by latitude.

### GRAPHICAL ABSTRACT



### ARTICLE INFO

Editor: Pavlos Kassomenos

#### Keywords:

Marine organic aerosol  
Shipborne measurement  
Latitudinal distribution  
Orbitrap mass spectrometry  
Ocean-sea ice-atmosphere interaction

### ABSTRACT

Sea spray aerosol (SSA) particles strongly influence clouds and climate but the potential impact of ocean microbiota on SSA fluxes is still a matter of active research. Here—by means of in situ ship-borne measurements—we explore simultaneously molecular-level chemical properties of organic matter (OM) in oceans, sea ice, and the ambient  $PM_{2.5}$  aerosols along a transect of 15,000 km from the western Pacific Ocean ( $36^{\circ}13'N$ ) to the Southern Ocean ( $75^{\circ}15'S$ ). By means of orbitrap mass spectrometry and optical characteristics, lignin-like material ( $24 \pm 5\%$ ) and humic material ( $57 \pm 8\%$ ) were found to dominate the pelagic Pacific Ocean surface, while intermediate conditions were observed in the Pacific-Southern Ocean waters. In the marine atmosphere, we found a gradient of features in the aerosol: lignin-like material ( $31 \pm 9\%$ ) dominating coastal areas and the pelagic Pacific Ocean, whereas lipid-like ( $23 \pm 16\%$ ) and protein-like ( $11 \pm 10\%$ ) OM controlled the sympagic Southern Ocean (sea ice-influence). The results of this study showed that the OM composition in the ocean, which changes with latitude, affects the OM in aerosol compositions in the atmosphere. This study highlights the importance of the global-scale OM monitoring of the close interaction between the ocean, sea ice, and the atmosphere. Sympagic primary marine aerosols in polar regions must be treated differently from other pelagic-type oceans.

### 1. Introduction

Considering that oceans cover approximately 70 % of the Earth's surface, marine surfaces containing large organic carbon pools can be a

\* Corresponding author.

E-mail address: [jypark@kopri.re.kr](mailto:jypark@kopri.re.kr) (J. Park).

<http://dx.doi.org/10.1016/j.scitotenv.2023.162969>

Received 24 November 2022; Received in revised form 7 March 2023; Accepted 16 March 2023

Available online 22 March 2023

0048-9697/© 2023 The Authors. Published by Elsevier B.V. This is an open access article under the CC BY license (<http://creativecommons.org/licenses/by/4.0/>).

substantial source of organic matter (OM) in aerosols, which is important in terms of carbon circulation between the ocean and atmosphere (Quinn et al., 2014). Marine OM in aerosols is emitted directly from the sea surface microlayer in the form of spray particles with high OM concentrations via the formation of a primary marine organic aerosol (Brooks and Thornton, 2018; Collins et al., 2014; O'Dowd and De Leeuw, 2007; Russell et al., 2010; Schmitt-Kopplin et al., 2012). Moreover, OM in aerosols can be generated from gaseous precursors produced by biological substances in the ocean (e.g., sulfuric acid, ammonia, halocarbons, isoprene, and monoterpenes) via nucleation in the atmosphere (secondary marine organic aerosol) (Barbaro et al., 2017; Kourtchev et al., 2014; Safi Shalamzari et al., 2013). Marine organic aerosols can significantly affect the global climate both directly (e.g., by scattering solar radiation) and indirectly (e.g., by regulating cloud formation), and their effects vary depending on the chemical properties of organic aerosols (Brooks and Thornton, 2018; Gantt et al., 2013; O'Dowd and De Leeuw, 2007; O'Dowd et al., 2004; Russell et al., 2010). Accordingly, the chemical properties of the OM in aerosols can play an important role in tracking the origin of the OM and effectively mitigating air pollution (Gantt et al., 2013). However, considering the importance of OM in aerosols and its impact on the climate, there is still a lack of research on the chemical properties and origins of organic aerosols. To investigate these comprehensively, it is necessary to analyze and directly compare the complex molecular properties of organic matter in the ocean and atmosphere (Brooks and Thornton, 2018).

Previous studies have reported that primary and secondary marine organic aerosols in the atmosphere are influenced by OM in various oceanic and coastal environments (Park et al., 2019; Park et al., 2022; Schmale et al., 2013; Zorn et al., 2008). For instance, the concentration of primary marine organic aerosols in the Korean and Arctic coastal systems, where river water is discharged, is positively correlated with the abundance of OM produced by marine biota (Park et al., 2019; Park et al., 2022). In addition, the concentration of OM in aerosols increases 20 times during the phytoplankton bloom event in the South Atlantic Ocean (Zorn et al., 2008). Meanwhile, OM in the ocean is widely distributed and has various chemical compositions under the influence of regional characteristics (e.g., latitude, ocean current, and land status). For example, OM in the ocean surrounding New Zealand is influenced by a number of major currents (Gonsior et al., 2008; Heath, 1985), resulting in a large input of terrestrial OM (Gonsior et al., 2011). In addition, potentially important sources of OM in the Southern Ocean are sea ice and land-based glacier systems (Hood et al., 2015), although clear mechanism has not yet been identified. This is because the OMs from sea ice and glacier are highly labile and bioavailable (Hood et al., 2009; Singer et al., 2012). A number of studies previously showed that the microbiota of sea ice and the sea ice-influenced ocean can be a source of atmospheric primary and secondary organic nitrogen, specifically low molecular weight alkylamines (Dall'Osto et al., 2022; Dall'Osto et al., 2017). Indeed, these organic nitrogen compounds should be considered when assessing secondary aerosol formation processes in Antarctica (Brean et al., 2021). Other follow-up studies also claim that the potential impact of the sea ice (sympagic) planktonic ecosystem on aerosol composition was overlooked in past studies, and multiple eco-regions act as distinct aerosol sources around Antarctica (Decesari et al., 2020; Rinaldi et al., 2020). Recently, Humphries et al. (2021) identified three main aerosol sources in the Southern Ocean: northern (40–45°S), mid-latitude (45–65°S), and Southern sector (65–70°S), with different mixture of continental and anthropogenic, primary, and secondary aerosols depending on the studied region. However, most studies on OM in aerosols have focused on specific regions and not in OM in the global ocean.

This work is significant in that we analyzed the OM properties in seawater, sea ice, and aerosols and investigated their interactions, especially on a global scale, at mid-high latitudes during a cruise. For this study, we simultaneously collected seawater, sea ice, and aerosol samples along a transect from the western Pacific Ocean (36°13'N) to the Southern Ocean (75°15'S) during the Korean icebreaker R/V *Araon* cruise. The main objectives of this study were: 1) to study the distributions and optical and molecular compositions of OM in the open ocean, sea ice, and atmosphere; and 2) to

investigate the OM relationship between the ocean and atmosphere by latitude. In this study, we attempted a more objective comparison of characteristics by exploring a wide research area along a long transect of 15,000 km from the western Pacific Ocean (36°13'N) to the Southern Ocean (75°15'S). The molecular-level characterization of OM in aerosols will allow us to better understand the ocean-sea ice-atmosphere interactions and the direction of various climate changes on a global scale.

## 2. Materials and methods

### 2.1. Seawater and sea ice samples

#### 2.1.1. Sample collection and pretreatment

In this study, 41 seawater samples were collected along a 15,000 km transect from the western Pacific Ocean (36°13'N) to the Southern Ocean (75°15'S) (Fig. 1) using the Korean Icebreaker R/V *Araon*. Seawater samples were collected from 20 stations in the western Pacific Ocean, excluding exclusive economic zones (EEZ) [between October 31st to November 28th and from December 19th to 20th, 2019, based on the Coordinated Universal Time (UTC)] (Table S1). Samples collected from stations (ST) 01–03 were classified as the west coast of Korea, whereas those collected from the Pacific Ocean were classified into three categories according to the nearest sea: the Philippine Sea (ST04–06), Western Equatorial Pacific Ocean (ST07–09), Tasman Sea (ST10–13), and sub-Antarctic zone (ST14–18 and ST45–46). From the Southern Ocean, 21 samples were collected along the round track of the ship to the Korean Antarctic Jang Bogo Station (74°37'S, 164°12'E) (from November 28th to December 19th, 2019, based on UTC) (Fig. 1). Samples collected from the Southern Ocean were classified into two categories: the Antarctic zone (ST19–24 and ST39–44) and the Ross Sea (ST25–38). All seawater samples were collected from a 7-m depth from the surface and immediately filtered using a 0.7- $\mu$ m filter (47 mm Glass Fiber Filter; GFF, Whatman, USA). The samples for orbitrap analysis were pretreated with solid-phase extraction (SPE) cartridges, as described in Section 2.1.3. Seawater temperature and salinity at the sampling stations were recorded using onboard temperature and salinity sensors.

Sea ice was detected in ST19 (61°30'S, 174°10'E) upon entering the Southern Ocean, and two sea ice fragments floating in the surface seawater of the Ross Sea were collected (74°37'S, 164°14'E). The sea ice concentration in the sampling area was approximately 45 %, according to the database of the National Snow and Ice Data Center (NSIDC). The thickness of the collected ice fragments was within 1-m with dark brown colored bottom as shown in Fig. S1. The collected sea ice samples were thawed and homogenized for pretreatment and storage, and then pretreated and stored using the same procedure as seawater for concentration, optical characteristics, and molecular-level chemical characteristics of OM.

#### 2.1.2. OM concentration and optical properties

The concentrations of dissolved organic carbon (DOC) were analyzed, and chromophoric and fluorescent dissolved organic matter (CDOM and FDOM, respectively) were measured for their optical properties. The detailed methods for these analyses are described in the Supplementary Information (Section S1).

#### 2.1.3. Solid phase extraction (SPE)

The filtered samples (550 mL to 10 L) were concentrated into a commercially available hydrophilic-lipophilic balanced (HLB) SPE cartridge (6 cc, 500 mg; Oasis-HLB, Waters, USA). The SPE pretreatment was conducted according to a method described in a previous study (Jang et al., 2020). Briefly, the concentrated OM in the SPE was eluted with 10 mL of methanol (HPLC grade; J.T. Baker, USA), which was stored at  $-20^{\circ}\text{C}$  during the ship track. The elution arriving at Korea was transferred to the laboratory under freezing conditions. Methanol was evaporated from the elution under gentle nitrogen gas, and then the concentrated OM in a final volume of 1 mL was treated with a 0.2- $\mu$ m pore size syringe filter (13 mm diameter; Advantec, Japan) to remove impurities.

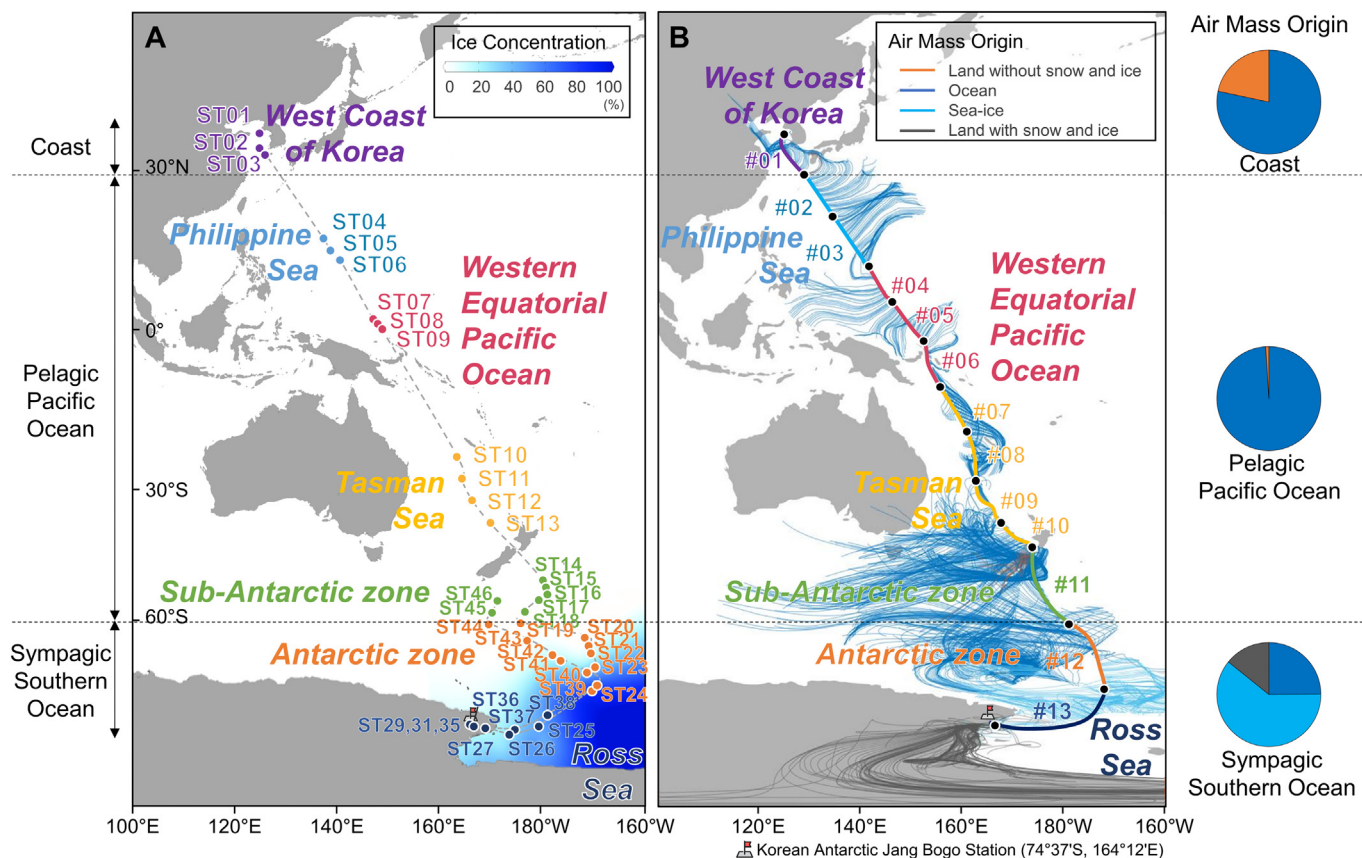


**Fig. 1.** (A) Sampling stations for OM of seawaters, with a ship track (dashed line) across the western Pacific and Southern Oceans. The relative concentrations of sea ice in NSIDC during sampling periods. (B) Sampling duration for OM in ambient aerosol along the ship track with three days air mass trajectories categorized into four main origins: land without snow and ice, ocean, sea ice, and land with snow and ice. Black dots denote boundaries for dividing sampling durations. The colors on the map show only one origin through which the air mass frequently passed, and the average value of all origins through which the air mass passed for three days is shown in a pie graph next to the map. The pie charts present relative components of the origins in the coast, pelagic- and sympagic oceans.

## 2.2. Aerosol samples

### 2.2.1. Sample collection and pretreatment

A total of 13 aerosol samples with equivalent aerodynamic diameters of  $<2.5 \mu\text{m}$  ( $\text{PM}_{2.5}$ ) were collected along transects from Korea to Jang Bogo Station (Fig. 1B). A high-volume air sampler (HV-1000R, Sibata Scientific Technology, Japan) installed at the compass deck (26-m above the bottom of the vessel) in front of the vessel was used to collect the aerosol samples.  $\text{PM}_{2.5}$  samples were collected in quartz filters (#2500 QAT-UP, Pall Life Sciences, USA), which were pre-combusted at 550 °C for 12 h to remove organic pollutants from the filters. Sampling was performed at a flow rate of 1000 L/min every 72 h. Following sampling, the quartz filter was packed immediately in aluminum foil and sealed completely into zipper bag, and then stored at  $-20 \text{ }^\circ\text{C}$  until analysis. Meteorological data such as air temperature, air pressure, wind speed, and wind direction were acquired through DaDiS which is an automatic observation and a primary data management system at R/V *Araon*.

### 2.2.2. OM concentration

Organic carbon (OC) concentrations were analyzed to quantitatively evaluate the properties of organic aerosols by latitude. The detailed methods for these analyses are described in the Supplementary Information (Section S1).

### 2.2.3. Solid phase extraction (SPE)

An area of approximately  $35 \text{ cm}^2$  was obtained from the filter using a punch and used to analyze the molecular compositions of the aerosol particles. Extraction was performed on a clean bench to minimize

contamination. The OM collected in the filter piece was dissolved in 20 mL of ultrapure water, and a bath sonicator was used for extraction. The OM dissolved in ultrapure water was concentrated using an SPE cartridge (1 cc, 30 mg; Oasis-HLB, Waters, USA) and then subjected to elution, solvent drying, and impurity removal processes such as those employed for seawater or ice samples to complete the pretreatment.

### 2.3. Orbitrap analysis and data processing

The conditions for the Orbitrap analysis are listed in Table S3. Liquid chromatography (LC)-Orbitrap-mass spectrometry (MS) was calibrated with Pierce™ ESI positive and negative ion calibration solutions before analysis to ensure high accuracy. As a blank for seawater and ice samples, ultrapure water was pretreated and analyzed in the same way as seawater, while an empty quartz filter with no samples collected was used as a blank for aerosols. The mass per charge ( $m/z$ ) and intensity for each peak from the mass spectrum were extracted using the MATLAB routine, and information on the formula was classified into C, H, O, N, and S. For each molecular formula allocated to evaluate the unsaturation and aromaticity, aromatic index (AI) was calculated (Koch and Dittmar, 2006). The van Krevelen diagrams were displayed using an FTMS Visualization package *i-van Krevelen* in Python 2.7, for subsequent analysis of the ranges  $0 < \text{H/C} < 2.5$ , and  $0 < \text{O/C} < 1.5$ . The molecular formulas in the van Krevelen diagrams were divided into seven categories based on previous study (Kim et al., 2003): lipid-like ( $\text{H/C} = 1.7\text{--}2.2$ ,  $\text{O/C} \leq 0.2$ ), protein-like ( $\text{H/C} = 1.5\text{--}2.0$ ,  $\text{O/C} = 0.2\text{--}0.6$ ), carbohydrate-like ( $\text{H/C} = 1.5\text{--}2.0$ ,  $\text{O/C} = 0.6\text{--}1.5$ ), unsaturated hydrocarbon-like ( $\text{H/C} = 0.6\text{--}1.5$ ,  $\text{O/C} \leq 0.1$ ), lignin-like ( $\text{H/C} = 0.6\text{--}1.5$ ,  $\text{O/C} = 0.1\text{--}0.6$ ,  $\text{AI} < 0.67$ ), tannin-like ( $\text{H/C} = 0.5\text{--}1.5$ ,  $\text{O/C} = 0.6\text{--}1.4$ ,  $\text{AI} < 0.67$ ), and condensed aromatic



structures ( $H/C \leq 0.7$ ,  $O/C \leq 0.4$ ,  $AI \geq 0.67$ ). The sum of the observed number and intensity of the assigned molecules can also be used as a semi-quantitative analysis method, reflecting a relatively quantitative aspect, because all samples were extracted from the same number of filters and analyzed under the same conditions.

#### 2.4. Hybrid Single Particle Lagrangian Integrated Trajectory (HYSPPLIT)

To determine the paths of the air mass, a back trajectory was calculated using the HYSPPLIT model over the collected time from mid-latitudes of the Northern Hemisphere to Jang Bogo station in the high-latitude of the Southern Hemisphere. The three-day back trajectory at 1 h intervals was calculated at an arrival height of 10 m above the ground along the ship track. The geographical information on ocean, land, and sea ice concentrations obtained from the NSIDC was combined with air mass back trajectories to calculate the percentage of the air mass retention time over the three terrain domains (Fig. 1B), as described by Jang et al. (2022) and Choi et al. (2019). The 13 aerosol samples were clustered with back trajectory data according to the hierarchical clustering algorithm by using the function *hclust* implemented in R (ver. 4.0.2).

#### 2.5. Statistical analysis

The samples were assessed using one-way analysis of variance (ANOVA). In the ANOVA, the *p*-value indicates the regional difference for each area; significant differences are considered to be represented by a *p*-value of  $<0.05$ . One-way ANOVA and *t*-test for post hoc analysis were calculated using SigmaPlot (Systat, USA).

### 3. Results and discussion

A total of 41 seawater samples were collected from seven regions of different part of our global oceans (i.e., west coast of Korea, Philippine Sea, Western Equatorial Pacific Ocean, Tasman Sea, sub-Antarctic zone, Antarctic zone, and Ross Sea). We categorized them in three main groups: coast, pelagic Pacific Ocean, and sympagic (sea ice influenced) Southern Ocean. The distances from adjacent land for the west coast of Korea were the closest in all sampling locations, especially for Korea ( $63 \pm 13$  km); thus, the west coast of Korea was separately classified as a coastal group, although it is included in the western Pacific Ocean. Meanwhile, five ocean samples except for the west coast of Korea are open oceans with  $904 \pm 440$  km distance from adjacent lands: the Philippine Sea, Western Equatorial Pacific Ocean, Tasman Sea, and sub-Antarctic zone are contained in the pelagic Pacific Ocean, while the Antarctic zone and the Ross Sea are categorized as the sympagic Southern Ocean due to the presence of sea ice.

#### 3.1. OM composition in the ocean

##### 3.1.1. Coast

High-resolution mass spectrum data are generally not quantitative; however, previous studies have successfully classified the main components of various types of natural organic matter (NOM) in the environment using the peak position of the van Krevelen diagram (Brogi et al., 2018; Choi et al., 2019; Kim et al., 2003; Longnecker, 2015; Stubbins et al., 2012; Wozniak et al., 2008). Additionally, the result of van Krevelen diagram analysis are consistent with those of nuclear magnetic resonance (NMR) analysis with respect to the qualitative identification of major compound classes included in the NOM samples (Kim et al., 2003). Thus, van Krevelen diagrams can be used to evaluate the relative significance of structurally related compounds and qualitatively classify them between samples (Choi et al., 2019; Kim et al., 2003).

In the west coast of Korea, the content of lignin-like OM was dominant ( $29 \pm 3$  %), followed by lipid-like ( $16 \pm 2$  %), protein-like ( $11 \pm 3$  %), condensed aromatic structures (CAS)-like ( $11 \pm 4$  %), unsaturated hydrocarbons (UH)-like ( $6 \pm 1$  %), tannin-like ( $5 \pm 3$  %), and carbohydrate-like OM ( $4 \pm 4$  %) (Fig. 2). Previous studies have reported

that lignin provide clear evidence of the terrestrial origin of OM (Hernes, 2003; Meyers-Schulte and Hedges, 1986), suggesting that OM in the west coast of Korea is largely influenced by land-derived OM. Moreover, in this study, terrestrial marker OMs, such as DOC concentrations, CAS-like, and tannin-like OMs, were higher in this region than in other seas, although the difference was not significant ( $p > 0.05$ ) (Table S1) (Hodgkins et al., 2014). The west coast of Korea is very close to land (Korea, Japan, and China; Table S1) and is considered to be an area affected by OM originating from land. Fig. 3 showed that the west coast of Korea is completely different with other oceans included in the pelagic Pacific Ocean and the sympagic Southern Ocean. The low salinity (especially 31.8 PSU at ST01) and high CDOM values (Fig. 3) indicate the influence of terrestrial sources. In addition, FDOM is one of the footprints for OM origins, and peak A, which represents terrestrial humic substances originating from terrestrial sources (Coble, 1996), was higher than that of the other seas (Fig. 3). Therefore, it seems that the OM in the west coast of Korea is of terrestrial-origin.

##### 3.1.2. Pelagic Pacific Ocean

Lipid-like OM was the most abundant in both the Philippine Sea and the Western Equatorial Pacific Ocean ( $28 \pm 9$  % and  $29 \pm 9$  %, respectively), followed by lignin-like (18–32 %), protein-like (10–14 %), UH-like (5–8 %), CAS-like (2–8 %), tannin-like (2–5 %), and carbohydrate-like OM (0–3 %) (Fig. 2; see Table S4 for content details). Lipid-like OM is generally of algal and/or microbial origins (Bhatia et al., 2010; Chen et al., 2003; Coble, 2007; Grannas et al., 2004; Pautler et al., 2011; Rontani et al., 2014; Schmidt et al., 2009), suggesting an increase in OM derived from marine plankton organisms and bacterial activity in these oceans. These OM characteristics are consistent with significantly higher protein characteristics of optical OM (peaks B and T) in the pelagic Pacific Ocean than in the sympagic Southern Ocean (Fig. 3). The peaks B and T are related to microbial activity, suggesting that OM in the pelagic Pacific Ocean is more affected by microorganisms than other oceanic regions studied. Owing to the North Equatorial Current heading west of the pelagic Pacific Ocean, the Philippine Sea and the Western Equatorial Pacific Ocean may be more affected by oceanic OM originating from the pelagic Pacific Ocean than by terrestrial OM originating from western lands. In the case of lignin-like OM, the content was  $24 \pm 7$  % in the Philippine Sea and  $22 \pm 3$  % in the Western Equatorial Pacific Ocean. In a previous study, the amount observed in the pelagic Pacific Ocean at similar latitudes ( $18^{\circ}47'N$ – $12^{\circ}19'S$ ;  $6.0$ – $14.2$  ng L<sup>-1</sup>) was 2.6 times lower than that observed in the Atlantic Ocean ( $24.9$ – $28.5$  ng L<sup>-1</sup>) (Opsahl and Benner, 1997). This was reported to be related to river discharge into the pelagic Pacific Ocean, which was 3.6 times lower than that of the Atlantic Ocean (Opsahl and Benner, 1997). Moreover, in this study, the sampling stations in the Philippine Sea and the Western Equatorial Pacific Ocean were far from lands up to 32 times compared to the distance between the west coast of Korea and adjacent land (Table S1). Another possibility for a lower lignin-like OM is photooxidation at surface seawaters. Previously, it has reported that photooxidation is the dominant factor influencing the composition and concentration of lignin, where salinity is above 25 PSU (Hernes, 2003). Moreover, the sampling depth in this study was within 7-m from surface which is included in the photic zone. Thus, we could suggest that relatively lower lignin content in the Philippine Sea and the Western Equatorial Pacific Ocean than the contents in the west coast of Korea ( $29 \pm 3$  %) may be due to increased photooxidation near the equator. Overall, the amount of lipid-like OM was 1.1–2.7 times higher and that of lignin-like OM was 1.0–1.7 times lower in the Philippine Sea and the Western Equatorial Pacific Ocean than those of the west coast of Korea. This is probably due to geological and chemical reasons such as ocean current, relatively low river discharge, far distance from terrestrial sources, and photooxidation.

Lignin-like and lipid-like OM contents were dominant in the Tasman Sea ( $23 \pm 2$  % and  $22 \pm 8$  %, respectively), followed by protein-like, UH-like, CAS-like, tannin-like, and carbohydrate-like OM (Fig. 2; see Table S4 for each content). Although lipid-like OM was lesser, protein-like OM was higher than those in the Philippine Sea and the Western

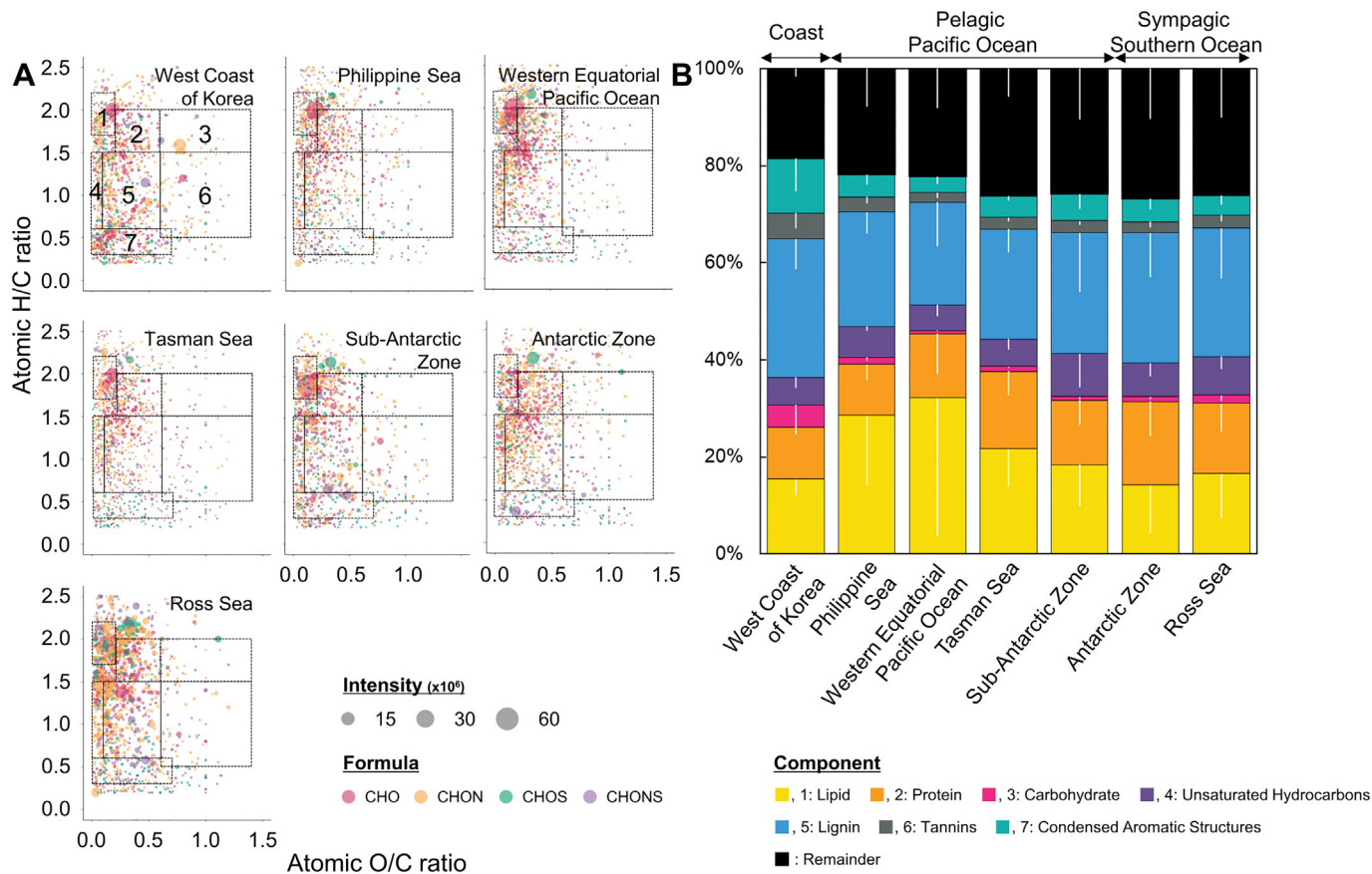


Fig. 2. (A) OM molecular composition on representative van Krevelen diagrams for seawater, and (B) the seven molecular compositions with relative abundances (%) of seawater. The relative abundances in each station are shown in Table S4.

Equatorial Pacific Ocean. Lipids and proteins have been reported as microbial origin-OM (Bhatia et al., 2010; Chen et al., 2003; Coble, 2007; Grannas et al., 2004; Pautler et al., 2011; Rontani et al., 2014; Schmidt et al., 2009), and marine phytoplankton have been reported to release polysaccharide-rich OM (e.g., heteropolysaccharides) and to accumulate them in the surface seawater as a result of metabolic resistance (Aluwihare and Repeta, 1999). Peaks B and T also differed from the sympagic Southern Ocean (Fig. 3), indicating that autochthonous and microbial OM is more actively generated in the pelagic Pacific Ocean than in the sympagic Southern Ocean. Interestingly, although the distance between sampling stations and adjacent lands was not significantly different between the Philippine Sea and the Western Equatorial Pacific Ocean, the contents of lignin-like OM, CDOM, and peak A in the Tasman Sea were similar and/or slightly lower than those of the Philippine Sea and the Western Equatorial Pacific Ocean (Figs. 2 and S1). These results are also shown in the optical properties in which terrestrial-origin OM markers, such as high CDOM and peak A values, were not detected (Fig. 3). Terrestrial OM characteristics such as the content of lignin-like OM, CDOM, and peak A in the Tasman Sea were lower than those in the west coast of Korea, where we found that the distance from land was significantly greater in the Tasman Sea than in the west coast of Korea ( $p < 0.05$ ). Hernes and Benner (2002) reported that lignin measurements in the pelagic Pacific Ocean could serve as a general tracer of river discharge and terrestrial OM in water masses. This was because the OM in the Tasman Sea was affected by terrestrial OM with the East Australia Current, which flows down the east coast of Australia and up the west coast of New Zealand (Hernes and Benner, 2002). In this study, we observed a consistent increase in lignin and tannin-like OM contents from ST10 to ST13 (sum of lignin-like and tannin-like OM contents: 23 % (ST10) → 23 % (ST11) → 26 % (ST12) → 28 % (ST13), Table S4). Therefore, both microbial activity and ocean currents seem to have a complex effect on OM composition in the Tasman Sea.

In the sub-Antarctic zone, lignin-like OM was the highest ( $24 \pm 5$  %), followed by lipid-like, protein-like, UH-like, CAS-like, tannin-like, and carbohydrate-like OM (Fig. 2; see Table S4 for each content). Interestingly, both molecular-level and optical properties showed boundary characteristics between the Tasman Sea and the Southern Ocean as shown in Figs. 2 and 3. The sub-Antarctic zone is a region where colder Antarctic seawater meets the relatively warmer seawater. Accordingly, the OM characteristics in the sub-Antarctic zone were likely affected by the OM derived from both pelagic and sympagic oceans.

### 3.1.3. Sympagic Southern Ocean

In both the Antarctic zone and the Ross Sea, lignin-like OM was the most dominant ( $27 \pm 6$  %), followed by lipid-like ( $14 \pm 9$  %) and protein-like OM ( $17 \pm 2$  %) (Fig. 2). Lignin has been reported to be transported by fronts and currents (Sarmiento and Quéré, 1996; Zangrando et al., 2019). The Southern Ocean changes from warm subtropical waters to cold polar waters through a variety of fronts and currents (e.g., subtropical front, sub-antarctic front, Antarctic polar front, and southern boundary of the Antarctic circular current) (Belkin and Gordon, 1996; Budillon and Rintoul, 2003; Honjo, 2004). For instance, there has been a large inflow of terrestrial OM into the western coast of New Zealand owing to a combination of intensive rainfall and dense rainforests (Gonsior et al., 2008). A substantial amount of OM was transported to the southeastern and eastern coasts of New Zealand along the ocean currents (Gonsior et al., 2011). Although the inflow and seasonal transport of land-derived OM to the ocean remain unclear, the inflow and transport of lignin-like OM to the Southern Ocean may have occurred in this study. Particularly, in Antarctica, OM, including lignin, has been reported to be transported and lifted to surface seawater by modified circulations and currents (e.g., the Antarctic circular current) (Sarmiento and Quéré, 1996; Zangrando et al., 2019). However, the higher content of lignin-like OM can be interpreted more effectively by FDOM results in

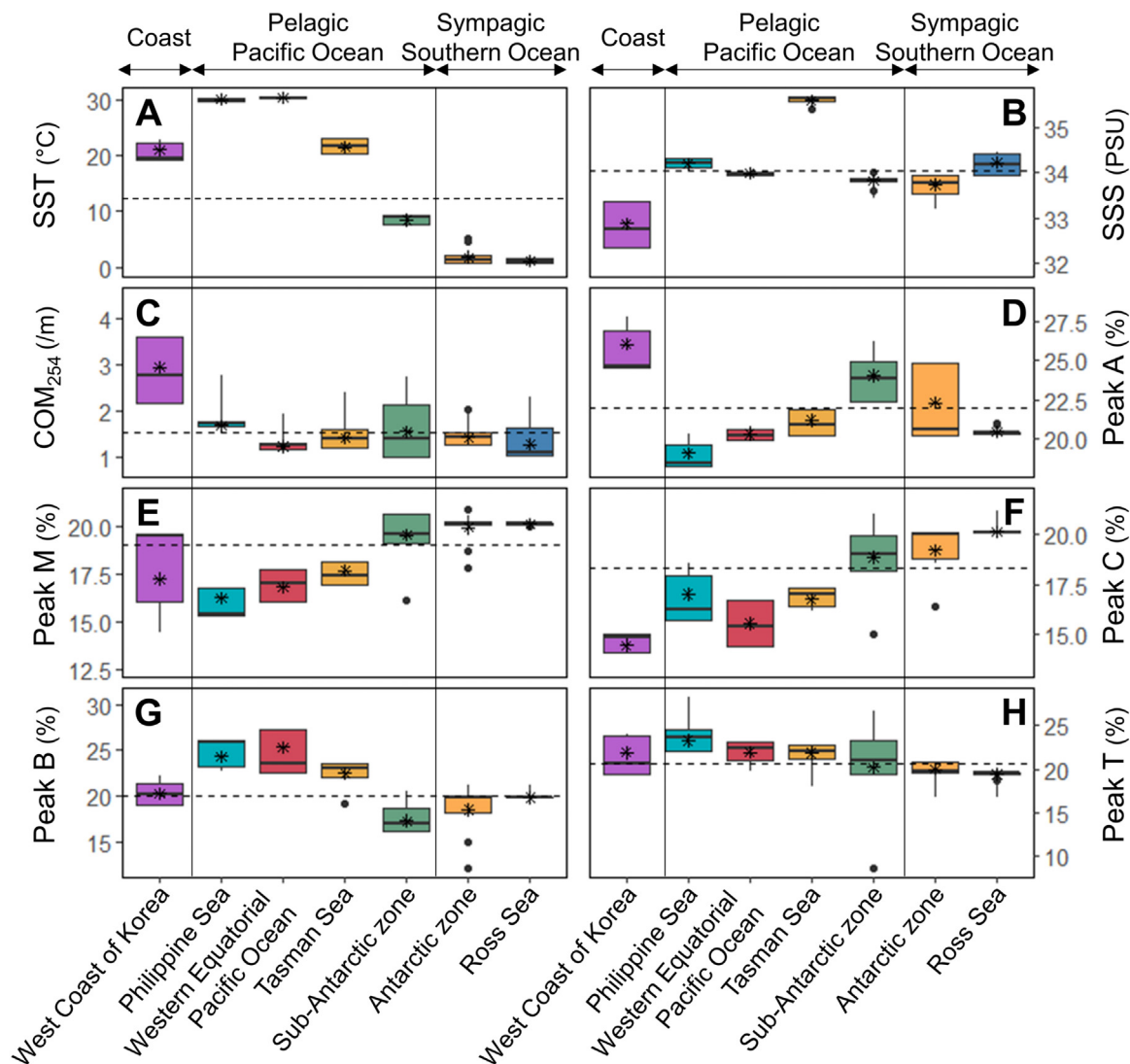


**Fig. 3.** Physical characteristics of seawaters: (A) sea surface temperature (SST), (B) sea surface salinity (SSS), (C) chromophoric OM (CDOM) absorption coefficient, and (D-H) relative fluorescence OM (FDOM) of surface seawater. Peaks A and C are generally classified as OM of terrestrial origin, peak M is known to be OM derived from marine humic or biological activity, and peaks B and T are classified as protein-like OMs derived from marine plankton organisms or bacteria (see Supplementary Information for details). The error bars refer to the standard deviation. Dashed-line presents the average.

the sympagic Southern Ocean (Fig. 3). Peak M is known to be humic OM of marine origin (Coble, 1996; Kopczyńska et al., 2001). Peak C is generally classified as humic of terrestrial origin; however, it has also been found in the oceans and is thus expected to be humic OM of marine origin (Coble, 1996; Coble et al., 1998; Stedmon and Markager, 2005). On the other hand, peaks B and T were reduced compared to other seas, suggesting that in the sympagic Southern Ocean, there was more marine humic-like OM and less protein-like OM than in the pelagic Pacific Ocean. Accordingly, since this study is based on qualitative analysis, it seems that the high content of lignin-like OM is a phenomenon caused by relatively few OM components due to low biological activities. Concisely, the OM in the sympagic Southern Ocean seems to have been more influenced by marine humic substances and biological reasons than by terrestrial sources.

### 3.2. OM composition in sea ice

Sea ice had a very different OM composition than the ocean, indicating a different origin. The molecular-level OM analysis of sea ice showed significant abundance of lipid-like OM ( $40 \pm 14\%$ ), which was the most prominent difference between sea ice and the ocean in terms of composition (Fig. 4). This result is consistent with the study that found significant

correlation between fatty acids and sea ice concentration in a sub-Antarctic Ice Core (King et al., 2019). In addition, protein-like OM (peak B + T =  $58 \pm 5\%$ ) was higher in sea ice than in oceans in terms of optical properties. These results coincide with previous study reported lipid and protein as the main organic compounds in Antarctic ice (D'Andrilli et al., 2010). Accordingly, based on the optical- and molecular-level OM results, the OM origins over the sea ice zone are estimated as follows: 1) microorganisms, 2) krill shrimp, and 3) atmospheric deposition. First, the dominant lipid content ( $O/C < 0.6$  and  $H/C > 1.7$ ) is consistent with the OM characteristics when green algae and/or microbes are actively present in sea ice (Bhatia et al., 2010; Grannas et al., 2004; Rontani et al., 2014; Schmidt et al., 2009). Specifically, Pusceddu et al. (1999) measured a lipid content of up to 68% in the biopolymer carbon flow collected from sediment cores under the ice pack of Terra Nova Bay in late summer. Moreover, the Ross Sea is the most biologically active region in Antarctica (D'Andrilli et al., 2010). Next, krill shrimp is a species that lives in the Southern Ocean, consumes plankton, and stores it in the form of lipids. Krill lipids are reported to increase by up to 10 times between summer and early winter (Pusceddu et al., 1999); therefore, the lipid content in sea ice is assumed to originate from krill lipids. Finally, it is possible that the lipids are the result of atmospheric deposition. Previous studies on the geological



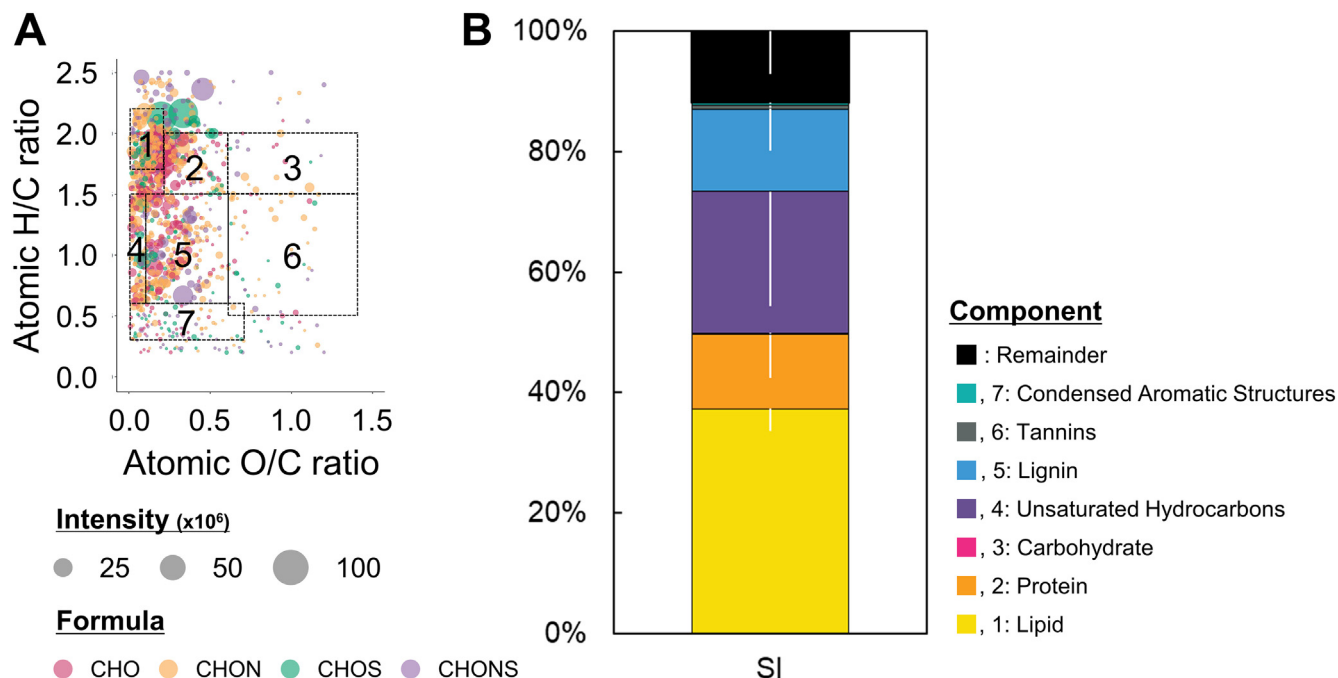


Fig. 4. (A) OM molecular composition on representative van Krevelen diagrams for sea ice (SI), and (B) the seven molecular compositions with relative abundances (%) of sea ice. The relative abundances in each station are shown in Table S4.

distribution of terrestrial plants in the Pacific have demonstrated that OM from terrestrial plants is easily transported over long distances, from neighboring continents to distant sea environments (Bendle et al., 2006; Ericson et al., 2018; Fang et al., 2002; Kawamura, 1995).

### 3.3. OM composition in ambient aerosol

In aerosol, lignin-like ( $31 \pm 10\%$ ) organic aerosols were dominant throughout the sampling stations, followed by lipid-like ( $14 \pm 8\%$ ), CAS-like ( $14 \pm 5\%$ ), protein-like ( $8 \pm 4\%$ ), tannin-like ( $7 \pm 4\%$ ), UH-like ( $6 \pm 2\%$ ), and carbohydrate-like ( $3 \pm 2\%$ ) organic aerosols (Table S4). To understand the molecular characteristics of OM in aerosols depending on the origin and pathway of air masses, three-day back trajectories were determined. We found that most air masses, except for those on the west coast of Korea and the Ross Sea, predominantly originated from oceans, with particularly higher ocean-originating air masses in the Philippine Sea, Western Equatorial Pacific Ocean, Tasman Sea, and sub-Antarctic zone ( $>90\%$ ) (Fig. 1). Nevertheless, some differences were observed in the ocean-originating air masses by latitude. For example, the Western Equatorial Pacific Ocean may have been affected by oceanic air masses for over three days; however, it is possible that these air masses were transported from the Indo-Pacific Islands for a rather short period before three days. Conversely, the air mass in the sub-Antarctic zone seemed to have originated from the ocean even before three days, and it was expected that the air masses would have entire oceanic aerosol properties. The west coast of Korea was categorized with the Philippine Sea, Western Equatorial Pacific Ocean, Tasman Sea, and sub-Antarctic zone in the air mass origin cluster with a high fraction of ocean-derived air mass (78%), although 22% of the air mass was originated from land (Fig. 5). Meanwhile, the Antarctic zone and the Ross Sea have been categorized as derived from similar air mass origin (i.e., sea ice) (Fig. 5). The air mass originated from sea ice (70%) and Antarctica (28%) in the case of the Ross Sea (Fig. 1), while in the Antarctic zone, a lesser fraction of air mass was derived from sea ice (52%).

The relative abundance of lignin-like organic aerosols was dominant from the west coast of Korea to the Antarctic zone (Fig. 6). In particular, the lignin-like organic aerosol content (49%) was the highest in the west coast of Korea. It indicates that this region was affected by land, which is

evident from its relatively closer distance to land ( $63 \pm 13$  km to Korea) and land-originating air mass being 15–50 times higher in this region than in other regions (except for the Ross Sea) (Fig. 1B). Moreover, higher OC concentrations were detected in the west coast of Korea ( $3.50 \mu\text{g}/\text{m}^3$ ) than in other sea areas ( $1.20 \pm 2.47 \mu\text{g}/\text{m}^3$ ) (Table S2). In previous studies, lignin-like organic aerosols have been reported as a proxy originating from land as a major residual component of decomposed vascular plants (Fang et al., 2002; Kawamura, 1995; Ohkouchi et al., 1997; Opsahl and Benner, 1997). For instance, the lignin concentration was 10 times higher in the

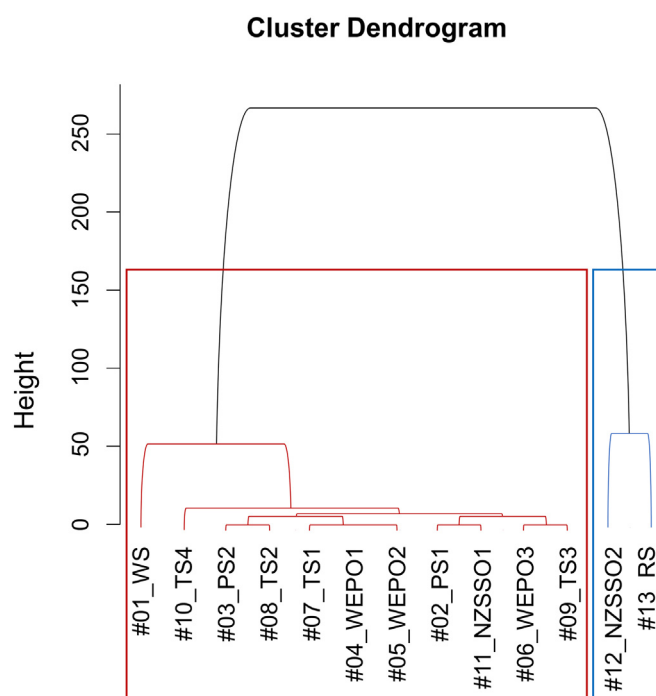


Fig. 5. Cluster analysis based on origins of the air mass. Units for height are dimensionless.

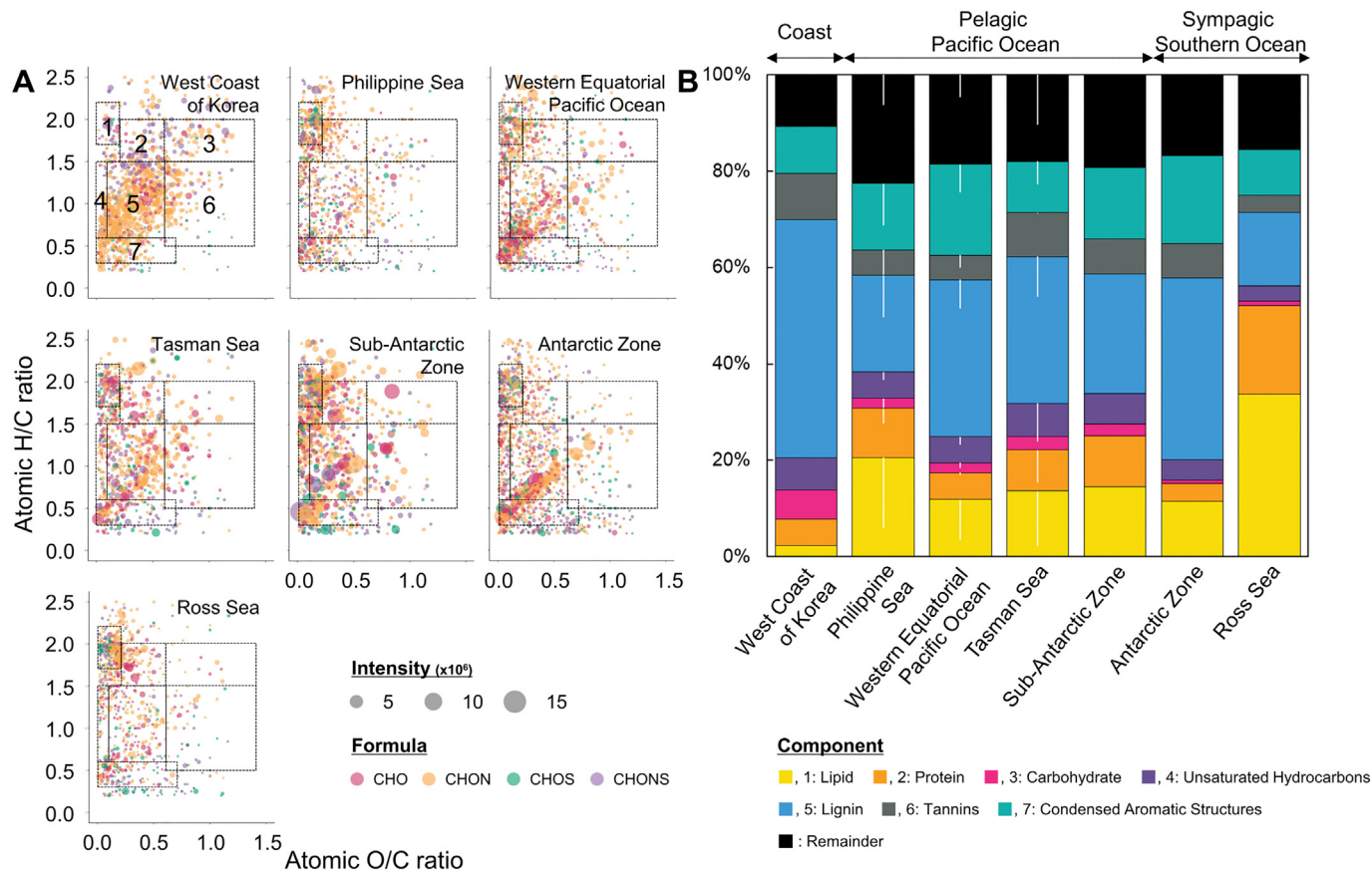


Fig. 6. (A) OM molecular composition on representative van Krevelen diagrams for ambient aerosol, and (B) the seven molecular compositions with relative abundances (%). The relative abundances in each station are shown in Table S5.

Arctic Ocean (100–300 km away from land), — which is generally affected by the Arctic River with 25 Tg of terrestrial OM per year, than in the Atlantic and Pacific Oceans (>3000 km away from land) (Kalbitz et al., 2006; Ohkouchi et al., 1997). Meanwhile, lignin-like organic aerosol content (19–41 %) dominated in the Philippine Sea, Western Equatorial Pacific Ocean, Tasman Sea, sub-Antarctic zone, and Antarctic zone, where the air masses mainly originated from the ocean ( $92 \pm 14$  %). The reason for lignin-like organic aerosols also being high in the Philippine Sea, Western Equatorial Pacific Ocean, Tasman Sea, sub-Antarctic zone, and Antarctic zone seems to be the hydrophobicity of lignin (Mitra et al., 2000). It is well-known that more hydrophobic particles become aerosolized better owing to their chemical selectivity (Dilling and Kaiser, 2002; Prather et al., 2013; Wang et al., 2017). In other words, hydrophobic particles in water are attracted to the air (bubble) and divided into an air-water interface (Dilling and Kaiser, 2002; Prather et al., 2013; Wang et al., 2017).

The content of lipid-like organic aerosol ranged from 2 % to 34 %, with slightly higher in the Philippine Sea, Western Equatorial Pacific Ocean, Tasman Sea, and sub-Antarctic zone (up to 23 %) than in the west coast of Korea (2 %). Most of the ocean-derived air masses ( $99 \pm 1$  %) originated from the region between the Philippine Sea and the sub-Antarctic zone. This seems to be due to the structural function of lipid, which is amphiphilic (both hydrophilic and hydrophobic properties) (Aller et al., 2005; Mitra et al., 2000). Accordingly, lipids have the potential to be aerosolized, although not as much as lignin. Interestingly, in the Ross Sea, unlike in other seas, the lipid-like organic aerosol was dominant (34 %), indicating that the ambient aerosol in the sympagic Southern Ocean is more affected by protein-like and lipid-like OM. The air mass mainly originated from sea ice (73 %) (Fig. 1B); therefore, it is assumed that sea ice is important in controlling the ambient aerosol chemical composition in the sympagic environment.

CAS-like organic aerosol distributed from 9 % to 25 % and was 2.6 times higher in the Philippine Sea, Western Equatorial Pacific Ocean, Tasman Sea, sub-Antarctic zone, and Antarctic zone than in the west coast of Korea and the Ross Sea. CAS has been reported to be derived mainly from anthropogenic sources (Wang et al., 2014) or land plants (Antony et al., 2014), and contributes to secondary organic aerosols (Wang et al., 2014). Accordingly, it is questionable why the content of CAS-like organic aerosols was the lowest in the west coast of Korea, where 22 % of air mass came from land. From the Philippine Sea to the Antarctic zone, where the air masses were predominantly derived from the ocean, CAS-like organic aerosols may have been transported for >72 h from anthropogenic sources or land. Indeed, a previous study reported that Antarctic aerosols containing CAS were related to black carbon travelling long distances for 10 days from South America, where active vegetation fires occurred (Antony et al., 2014; Gurganus et al., 2015). Meanwhile, protein-like, carbohydrate-like, UH-like, and tannin-like organic aerosols had very low average contents of approximately 10 % in each sea, and there was no significant difference among the seas.

### 3.4. Implication of the linkage between the ocean, sea ice, and the atmosphere in different regions

The contents of the OM components in both the ocean and aerosol were compared for each sea (Fig. 7A). Lignin-like OM was clearly dominant in both seawater and aerosol of both the west coast of Korea and the Antarctic zone. In particular, in the west coast of Korea, seawater and aerosol had higher lignin-like OM content than other oceans, suggesting that certainly much more terrestrial OM affect to chemical composition of the atmosphere when air mass was relatively more came from lands. In the Philippine Sea, Western Equatorial Pacific Ocean, and Tasman Sea, lipid-



like OM was slightly higher than lignin-like OM in the ocean, whereas lignin-like organic aerosol was dominant in the atmosphere. This suggests that lignin-like OM could be more aerosolized compared to lipid-like OM in the ocean. This is because lignin is more hydrophobic than lipids, which have amphiphilic properties (Aller et al., 2005; Mitra et al., 2000). Indeed, research on plant extracts has shown that the hydrophobicity of lignin is 5.4 times higher than that of lipids in terms of hydrophobic solvent sorption and octanol-water partitioning coefficients (Chen and Schnoor, 2009). Remarkably, in the Ross Sea, the lipid-like organic aerosol content was predominant in the atmosphere, even though the lignin-like OM component was more dominant in the ocean. Accordingly, to determine the influence of sea ice on aerosol, a comparison between the OM content in sea ice and aerosol was performed (Fig. 7B). The highest contents of lipid-like OM in both sea ice and aerosol suggest that the OM characteristics of aerosol in the Ross Sea would have been influenced by OM in sea ice. Indeed,  $35 \pm 29\%$  of the seawater surface in the Ross Sea was covered with sea ice (Fig. 1A), and the air mass mainly originated from sea ice, unlike other seas. A higher portion of lipid-like organic aerosol of the Ross Sea may have been 1) aerosolized by sea ice-related processes (e.g., the atmospheric oxidation of lipids or wind-blown effect) or 2) melted into the ocean and then aerosolized directly from the ocean into the atmosphere via the bubble bursting process. In the former case, a high abundance of lipid substances (e.g., carboxyl acid) was released into the Arctic atmosphere with sea ice contributions (Feltracco et al., 2021). For instance, Feltracco et al. (2021) showed that high concentrations of long-chain carboxyl acids (e.g., adipic and pimelic acids), which are oxidized forms of lipids, were accompanied by relatively high bromine and iodine concentrations. Moreover, long-chain carboxyl acids were regulated by emissions linked to sub-ice algal populations (Kawamura et al., 1996). Although no mechanism for lipid aerosolization from sea ice has been clearly identified, we hypothesized that the lipid components released by sea ice may be oxidized to produce lipid-like organic aerosol in the atmosphere of the Ross Sea site. In addition to the atmospheric oxidation of lipids, results for aerosolizing sea salt by wind blowing have been reported for sea ice (Jones et al., 2009; Lieb-Lappen and Obbard, 2015; May et al., 2016; Russell et al., 2010; Yang et al., 2019; Yang et al., 2008). Previous studies have reported that the aerosolization of sea salt or bromine compounds on sea ice or snow was related to a wind speed of 4–10 m/s (Jones et al., 2009; Lieb-Lappen and Obbard, 2015; May et al., 2016; Yang et al., 2019; Yang et al., 2008). In this study, the wind speed was 1.3–11.7 ( $3.8 \pm 2.8$ ) m/s during sampling in the Ross Sea (Table S2), which may have led to sufficient

particles or OM on the sea ice surface to aerosolize. Thus, we speculated the possibility that lipid-like OM was aerosolized directly on the sea ice surface by wind, although more research is required due to the differences of aerosol size between this study ( $<0.45 \mu\text{m}$ ) and previous studies ( $0.4$  to  $12 \mu\text{m}$ ) (Jones et al., 2009; Lieb-Lappen and Obbard, 2015; May et al., 2016; Yang et al., 2019; Yang et al., 2008). Moreover, Rhodes et al. (2017) reported simulation results that only the amount of aerosol generated in the ocean was insufficient compared to observations, thus suggesting that aerosol generated from sea ice should be considered. In the latter case, lipid-containing aerosol is expected to be transported from the ocean to the atmosphere (Ceburnis et al., 2016; Decesari et al., 2020; Liu et al., 2018). However, lignin-like OM was dominant in the seawater of the Ross Sea, indicating that the effect of lipids from melting sea ice would not have been significant. The salinity ( $34 \pm 0.3$  PSU) of the Ross Sea did not decrease substantially during the sampling period of this study (i.e., late November to early December), implying that seawater in the Ross Sea was not considerably affected by the meltwater from sea ice. A previous study reported that salinity lower than 34.0 PSU was observed when affected by meltwater on the coast of Antarctica (Alderkamp et al., 2015). Therefore, this study focused on the possibility of the former case, in which lipid-like organic aerosols were aerosolized from sea ice into the atmosphere due to the atmospheric oxidation of lipids or the wind-blown effect. Further studies are necessary to better understand sea ice-related processes.

As shown in Fig. S5, there was no significant correlation for most of the OM components, except for carbohydrate-like ( $r^2 = 0.56, p < 0.1$ ) and UH-like OM ( $r^2 = 0.34, p < 0.05$ ), suggesting that the effect of OM in the ocean on OM in aerosol does not correlate with latitude. Nevertheless, Fig. S6 clearly showed that lipid-like and protein-like OM were very high in the Ross Sea aerosol, emphasizing that lipid and protein are important compositions that regulate the organic aerosol components of the Ross Sea. Carbohydrate-like OM showed no significant correlation with other oceans, except for the west coast of Korea, where an unusually high carbohydrate-like OM content was detected in both the ocean and aerosols. Although the overall carbohydrate content in the aerosols was lower than 6%, that in the pelagic Pacific Ocean was higher than that in the sympagic Southern Ocean. The UH-like OM component showed a negative correlation between seawater and aerosols; however, this observation was inconsistent with latitude, suggesting that the correlation between UH-like OM components of the ocean and atmosphere may be independent of latitude. Thus, these results indicate that the specific chemical composition of OM may affect the relationship between the ocean and atmosphere.

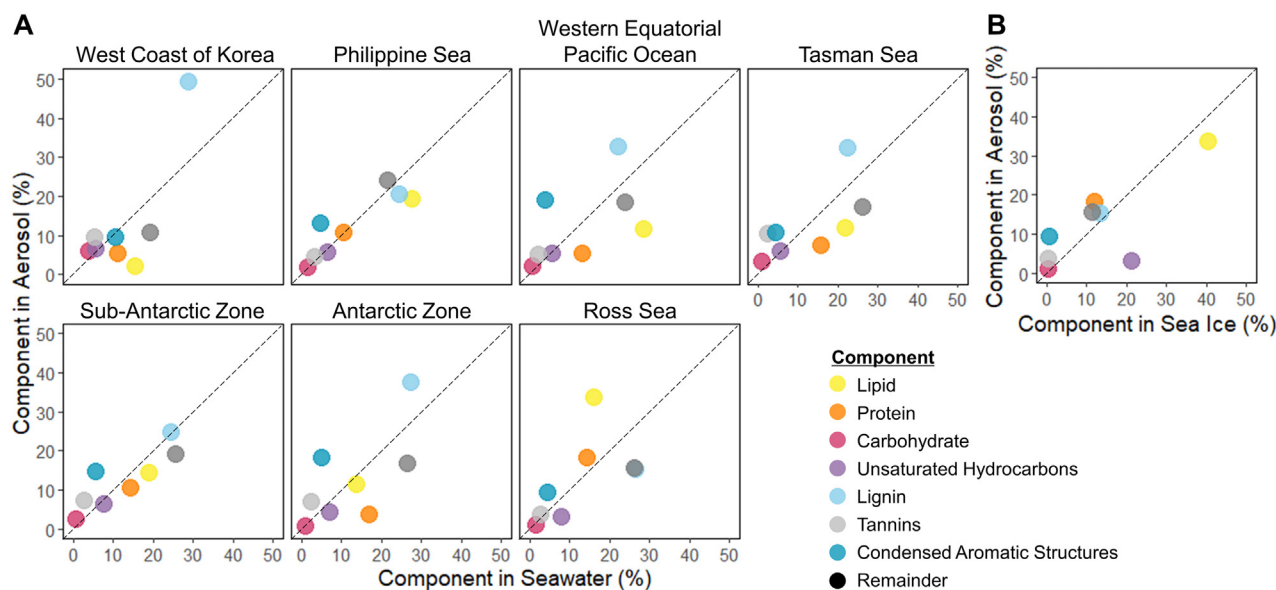


Fig. 7. The components shared (A) between seawater and aerosol samples, and (B) between sea ice and aerosol samples. Each dot represents averaged content at each ocean.

#### 4. Conclusions

The results of this study suggested the ocean-atmosphere interactions by providing the molecular properties of OM in the ocean, sea ice, and atmosphere based on data obtained from a cruise of a 15,000 km transect from the western Pacific Ocean to the Southern Ocean. Except for the Ross Sea, lignin-like OM was dominant in the atmosphere, suggesting that OM in aerosols can be controlled by OM in the ocean. In contrast, the air mass mainly originated from sea ice in the Ross Sea, and the relationship between sea ice and aerosol was found by compositional similarity dominated by lipid-like OM.

This study highlights the global importance of the lignin-like and lipid-like OM. Lignin-like OM is an important component of the open ocean. Previous studies on various oceans, including the Pacific Ocean, have reported carboxylic-rich alicyclic molecules containing lignin-like OM are the most dominant OM (40–65 %) (Chen et al., 2014; Kellerman et al., 2018; Schmidt et al., 2017). In addition, OMs are released directly from surface seawater to the atmosphere through bubble bursting (Brooks and Thornton, 2018; O'Dowd and De Leeuw, 2007; Schmitt-Kopplin et al., 2012), and in particular, lignin-like OM can be released more than other OM types owing to its higher hydrophobicity. Considering that the ocean accounts for 70 % of the Earth's surface, the amount and effect of lignin-like OM in the ocean on the atmosphere should not be ignored. Additionally, lignin in aerosol has been shown to produce colored organic species by reacting with OH radicals in a model study (Hoffer et al., 2004). These species play an important role in the atmospheric absorption of solar radiation because they have a stronger absorption capacity in the lower range than UV (Hoffer et al., 2004). In this study, we provided significant results on ocean-atmosphere interactions by latitude through ratios of chemical characteristics, not quantitative results. Accordingly, more research is required to determine the amount of lignin-like OM transported from the ocean to the atmosphere and how it affects the atmosphere.

In Antarctic ocean, lipid-like organic aerosols are expected to decrease by the sea ice OM properties in the case of the reduction of the Antarctic sea ice area. Indeed, the Antarctic sea ice area has been declining since 2016, reaching its lowest point in 2022, which is equivalent to 30 years of Arctic sea ice loss (Eayrs et al., 2021; Raphael and Handcock, 2022). Accordingly, in the future, it is hypothesized that the characteristics of OM in aerosols in the Antarctic atmosphere may more accurately reflect the OM characteristics of the ocean (i.e., lignin-like OM) than those of sea ice (i.e., lipid-like OM). These changes in OM in aerosol characteristics can play an important role in climate change on both regional and global scales. Therefore, research should continue to explore the OM distribution in oceans globally, including the Arctic and Antarctic regions, where sea ice exists, as well as to understand the impact on OM in aerosols.

#### CRedit authorship contribution statement

**Jiyi Jang:** Investigation, Writing – original draft, Visualization. **Jiyeon Park:** Conceptualization, Writing – original draft, Supervision. **Jongkwan Park:** Methodology, Writing – review & editing. **Young Jun Yoon:** Writing – review & editing. **Manuel Dall'Osto:** Writing – review & editing. **Ki-Tae Park:** Writing – review & editing. **Eunho Jang:** Formal analysis, Data curation. **Ji Yi Lee:** Writing – review & editing. **Kyung Hwa Cho:** Writing – review & editing. **Bang Yong Lee:** Writing – review & editing, Funding acquisition.

#### Data availability

Data will be made available on request.

#### Declaration of competing interest

The authors declare that they have no known competing financial interests or personal relationships that could have appeared to influence the work reported in this paper.

#### Acknowledgments

This research was supported by KOPRI projects (PE23030) and partly supported by grants from the Korean Government (MSIT) (NRF-2021M1A5A1065425, KOPRI-PN23011). And we are grateful to the captain and crew of the R/V *Araon* for their enthusiastic assistance during the study.

#### Appendix A. Supplementary data

Supplementary data to this article can be found online at <https://doi.org/10.1016/j.scitotenv.2023.162969>.

#### References

- Alderkamp, A.-C., Van Dijken, G.L., Lowry, K.E., Connelly, T.L., Lagerström, M., Sherrell, R.M., et al., 2015. Fe availability drives phytoplankton photosynthesis rates during spring bloom in the Amundsen Sea polynya, Antarctica. *Fe availability drives photosynthesis in Amundsen Sea polynya*. *Elementa* (Wash. D.C.) 3.
- Aller, J.Y., Kuznetsova, M.R., Jahns, C.J., Kemp, P.F., 2005. The sea surface microlayer as a source of viral and bacterial enrichment in marine aerosols. *J. Aerosol Sci.* 36, 801–812. <https://doi.org/10.1016/j.jaerosci.2004.10.012>.
- Aluwihare, L.I., Repeta, D.J., 1999. A comparison of the chemical characteristics of oceanic DOM and extracellular DOM produced by marine algae. *Mar. Ecol. Prog. Ser.* 186, 105–117.
- Antony, R., Grannas, A.M., Willoughby, A.S., Sleighter, R.L., Thamban, M., Hatcher, P.G., 2014. Origin and sources of dissolved organic matter in snow on the East Antarctic ice sheet. *Environ. Sci. Technol.* 48, 6151–6159. <https://doi.org/10.1021/es405246a>.
- Barbaro, E., Padoan, S., Kirchgorg, T., Zangrando, R., Toscano, G., Barbante, C., et al., 2017. Particle size distribution of inorganic and organic ions in coastal and inland Antarctic aerosol. *Environ. Sci. Pollut. Res.* 24, 2724–2733. <https://doi.org/10.1007/s11356-016-8042-x>.
- Belkin, I.M., Gordon, A.L., 1996. Southern ocean fronts from the Greenwich meridian to Tasmania. *J. Geophys. Res. Oceans* 101, 3675–3696. <https://doi.org/10.1029/95jc02750>.
- Bendle, J.A., Kawamura, K., Yamazaki, K., 2006. Seasonal changes in stable carbon isotopic composition of n-alkanes in the marine aerosols from the western North Pacific: implications for the source and atmospheric transport. *Geochim. Cosmochim. Acta* 70, 13–26. <https://doi.org/10.1016/j.gca.2005.08.013>.
- Bhatia, M.P., Das, S.B., Longnecker, K., Charette, M.A., Kujawinski, E.B., 2010. Molecular characterization of dissolved organic matter associated with the Greenland ice sheet. *Geochim. Cosmochim. Acta* 74, 3768–3784. <https://doi.org/10.1016/j.gca.2010.03.035>.
- Brean, J., Dall'Osto, M., Simó, R., Shi, Z., Beddows, D.C.S., Harrison, R.M., 2021. Open ocean and coastal new particle formation from sulfuric acid and amines around the Antarctic Peninsula. *Nature Geoscience* 14, 383–388. <https://doi.org/10.1038/s41561-021-00751-y>.
- Brooks, S.D., Thornton, D.C., 2018. Marine aerosols and clouds. *Annu. Rev. Mar. Sci.* 10, 289–313.
- Broggi, S.R., Ha, S.-Y., Kim, K., Derrien, M., Lee, Y.K., Hur, J., 2018. Optical and molecular characterization of dissolved organic matter (DOM) in the Arctic ice core and the underlying seawater (Cambridge Bay, Canada): implication for increased autochthonous DOM during ice melting. *Sci. Total Environ.* 627, 802–811. <https://doi.org/10.1016/j.scitotenv.2018.01.251>.
- Budillon, G., Rintoul, S.R., 2003. Fronts and upper ocean thermal variability south of New Zealand. *Antarct. Sci.* 15, 141–152. <https://doi.org/10.1017/S09594102003001135>.
- Ceburnis, D., Masalaite, A., Ovadnevaite, J., Garbaras, A., Remeikis, V., Maenhaut, W., et al., 2016. Stable isotopes measurements reveal dual carbon pools contributing to organic matter enrichment in marine aerosol. *Sci. Rep.* 6, 36675. <https://doi.org/10.1038/srep36675>.
- Chen, B., Schnoor, J.L., 2009. Role of suberin, suberan, and hemicellulose in phenanthrene sorption by root tissue fractions of switchgrass (*Panicum virgatum*) seedlings. *Environ. Sci. Technol.* 43, 4130–4136. <https://doi.org/10.1021/es803510u>.
- Chen, H., Stubbins, A., Perdue, E.M., Green, N.W., Helms, J.R., Mopper, K., et al., 2014. Ultra-high resolution mass spectrometric differentiation of dissolved organic matter isolated by coupled reverse osmosis-electrodialysis from various major oceanic water masses. *Mar. Chem.* 164, 48–59. <https://doi.org/10.1016/j.marchem.2014.06.002>.
- Chen, W., Westerhoff, P., Leenheer, J.A., Booksh, K., 2003. Fluorescence excitation – emission matrix regional integration to quantify spectra for dissolved organic matter. *Environ. Sci. Technol.* 37, 5701–5710. <https://doi.org/10.1021/es034354c>.
- Choi, J., Jang, E., Yoon, Y., Park, J., Kim, T.W., Becagli, S., et al., 2019. Influence of biogenic organics on the chemical composition of Arctic aerosols. *Glob. Biogeochem. Cycles* 33, 1238–1250. <https://doi.org/10.1029/2019gb006226>.
- Coble, P.G., 1996. Characterization of marine and terrestrial DOM in seawater using excitation-emission matrix spectroscopy. *Mar. Chem.* 51, 325–346. [https://doi.org/10.1016/0304-4203\(95\)00062-3](https://doi.org/10.1016/0304-4203(95)00062-3).
- Coble, P.G., 2007. Marine optical biogeochemistry: the chemistry of ocean color. *Chem. Rev.* 107, 402–418. <https://doi.org/10.1021/cr050350+>.
- Coble, P.G., Del Castillo, C.E., Avril, B., 1998. Distribution and optical properties of CDOM in the Arabian Sea during the 1995 southwest monsoon. *Deep-Sea Res. II Top. Stud. Oceanogr.* 45, 2195–2223. [https://doi.org/10.1016/S0967-0645\(98\)00068-X](https://doi.org/10.1016/S0967-0645(98)00068-X).
- Collins, D., Zhao, D., Ruppel, M., Laskina, O., Grandquist, J., Modini, R., et al., 2014. Direct aerosol chemical composition measurements to evaluate the physicochemical differences

- between controlled sea spray aerosol generation schemes. *Atmos. Meas. Tech.* 7, 3667–3683. <https://doi.org/10.5194/amt-7-3667-2014>.
- D'Andrilli, J., Dittmar, T., Koch, B.P., Purcell, J.M., Marshall, A.G., Cooper, W.T., 2010. Comprehensive characterization of marine dissolved organic matter by fourier transform ion cyclotron resonance mass spectrometry with electrospray and atmospheric pressure photoionization. *Rapid Commun. Mass Spectrom.* 24, 643–650. <https://doi.org/10.1002/rcm.4421>.
- Dall'Osto, M., Ovadnevaite, J., Paglione, M., Beddows, D.C.S., Ceburnis, D., Cree, C., et al., 2017. Antarctic sea ice region as a source of biogenic organic nitrogen in aerosols. *Sci. Rep.*, 7 <https://doi.org/10.1038/s41598-017-06188-x>.
- Dall'Osto, M., Vaqué, D., Sotomayor-García, A., Cabrera-Brufau, M., Estrada, M., Buchaca, T., et al., 2022. Sea ice microbiota in the Antarctic Peninsula modulates cloud-relevant sea spray aerosol production. *Front. Mar. Sci.* 9. <https://doi.org/10.3389/fmars.2022.827061>.
- Decesari, S., Paglione, M., Rinaldi, M., Dall'Osto, M., Simó, R., Zanca, N., et al., 2020. Shipborne measurements of Antarctic submicron organic aerosols: an NMR perspective linking multiple sources and bioregions. *Atmos. Chem. Phys.* 20, 4193–4207. <https://doi.org/10.5194/acp-20-4193-2020>.
- Dilling, J., Kaiser, K., 2002. Estimation of the hydrophobic fraction of dissolved organic matter in water samples using UV photometry. *Water Res.* 36, 5037–5044. [https://doi.org/10.1016/S0043-1354\(02\)00365-2](https://doi.org/10.1016/S0043-1354(02)00365-2).
- Eayrs, C., Li, X., Raphael, M.N., Holland, D.M., 2021. Rapid decline in Antarctic sea ice in recent years hints at future change. *Nat. Geosci.* 14, 460–464. <https://doi.org/10.1038/s41561-021-00768-3>.
- Ericson, J.A., Hellesey, N., Nichols, P.D., Kawaguchi, S., Nicol, S., Hoem, N., et al., 2018. Seasonal and interannual variations in the fatty acid composition of adult *Euphausia superba* Dana, 1850 (Euphausiacea) samples derived from the Scotia Sea krill fishery. *J. Crustac. Biol.* <https://doi.org/10.1093/jcbiol/ruy032>.
- Fang, J., Kawamura, K., Ishimura, Y., Matsumoto, K., 2002. Carbon isotopic composition of fatty acids in the marine aerosols from the Western North Pacific: implication for the source and atmospheric transport. *Environ. Sci. Technol.* 36, 2598–2604. <https://doi.org/10.1021/es015863m>.
- Feltracco, M., Barbaro, E., Spolario, A., Vecchiato, M., Callegaro, A., Burgay, F., et al., 2021. Year-round measurements of size-segregated low molecular weight organic acids in Arctic aerosol. *Sci. Total Environ.* 763, 142954. <https://doi.org/10.1016/j.scitotenv.2020.142954>.
- Gantt, B., Meskhidze, N.J.A.C., Physics, 2013. The physical and chemical characteristics of marine primary organic aerosol: a review. *Atmospheric Chemistry and Physics* 13, 3979–3996. <https://doi.org/10.5194/acp-13-3979-2013>.
- Gonsior, M., Peake, B.M., Cooper, W.T., Jaffé, R., Young, H., Kahn, A.E., et al., 2008. Spectral characterization of chromophoric dissolved organic matter (CDOM) in a fjord (Doubtful sound, New Zealand). *Aquat. Sci.* 70, 397–409.
- Gonsior, M., Peake, B.M., Cooper, W.T., Podgorski, D.C., D'Andrilli, J., Dittmar, T., et al., 2011. Characterization of dissolved organic matter across the subtropical convergence off the South Island, New Zealand. *Mar. Chem.* 123, 99–110. <https://doi.org/10.1016/j.marchem.2010.10.004>.
- Grannas, A.M., Shepson, P.B., Filley, T.R., 2004. Photochemistry and nature of organic matter in Arctic and Antarctic snow. *Glob. Biogeochem. Cycles* 18, Gb1006. <https://doi.org/10.1029/2003gb002133>.
- Gurganus, S.C., Wozniak, A.S., Hatcher, P.G., 2015. Molecular characteristics of the water soluble organic matter in size-fractionated aerosols collected over the North Atlantic Ocean. *Mar. Chem.* 170, 37–48. <https://doi.org/10.1016/j.marchem.2015.01.007>.
- Heath, R.A., 1985. A review of the physical oceanography of the seas around New Zealand—1982. *N. Z. J. Mar. Freshw. Res.* 19, 79–124. <https://doi.org/10.1080/00288330.1985.9516077>.
- Hernes, P.J., 2003. Photochemical and microbial degradation of dissolved lignin phenols: implications for the fate of terrigenous dissolved organic matter in marine environments. *J. Geophys. Res.* 108. <https://doi.org/10.1029/2002jc001421>.
- Hernes, P.J., Benner, R., 2002. Transport and diagenesis of dissolved and particulate terrigenous organic matter in the North Pacific Ocean. *Deep-Sea Res. I Oceanogr. Res. Pap.* 49, 2119–2132. [https://doi.org/10.1016/S0967-0637\(02\)00128-0](https://doi.org/10.1016/S0967-0637(02)00128-0).
- Hodgkins, S.B., Traily, M.M., McCalley, C.K., Logan, T.A., Crill, P.M., Saleska, S.R., Rich, V.I., Chanton, J.P., 2014. Changes in peat chemistry associated with permafrost thaw increase greenhouse gas production. *Proc. Natl. Acad. Sci. U. S. A.* 111 (16), 5819–5824. <https://doi.org/10.1073/pnas.1314641111>.
- Hoffer, A., Kiss, G., Blazsó, M., Gelencsér, A., 2004. Chemical characterization of humic-like substances (HULIS) formed from a lignin-type precursor in model cloud water. *Geophys. Res. Lett.* 31, n/a–n/a. <https://doi.org/10.1029/2003gl018962>.
- Honjo, S., 2004. Particle export and the biological pump in the Southern Ocean. *Antarct. Sci.* 16, 501–516. <https://doi.org/10.1017/S0954102004002287>.
- Hood, E., Battin, T.J., Fellman, J., O'Neil, S., Spencer, R.G.M., 2015. Storage and release of organic carbon from glaciers and ice sheets. *Nat. Geosci.* 8, 91–96. <https://doi.org/10.1038/ngeo2331>.
- Hood, E., Fellman, J., Spencer, R.G.M., Hernes, P.J., Edwards, R., D'Amore, D., et al., 2009. Glaciers as a source of ancient and labile organic matter to the marine environment. *Nature* 462, 1044–1047. <https://doi.org/10.1038/nature08580>.
- Humphries, R.S., Keywood, M.D., Gribben, S., McRobert, I.M., Ward, J.P., Selleck, P., et al., 2021. Southern Ocean latitudinal gradients of cloud condensation nuclei. *Atmos. Chem. Phys.* 21, 12757–12782. <https://doi.org/10.5194/acp-21-12757-2021>.
- Jang, E., Park, K.-T., Yoon, Y.J., Kim, K., Gim, Y., Chung, H.Y., et al., 2022. First-Year Sea ice leads to an increase in dimethyl sulfide-induced particle formation in the Antarctic peninsula. *Sci. Total Environ.* 803, 150002. <https://doi.org/10.1016/j.scitotenv.2021.150002>.
- Jang, J., Park, J., Ahn, S., Park, K.-T., Ha, S.-Y., Park, J., Cho, K.H., 2020. Molecular-level chemical characterization of dissolved organic matter in the ice shelf systems of the King George Island Antarctica. *Front Mar Sci* 7 (339), 339. <https://doi.org/10.3389/fmars.2020.00339>.
- Jones, A.E., Anderson, P.S., Begoin, M., Brough, N., Hutterli, M.A., Marshall, G.J., et al., 2009. BrO, blizzards, and drivers of polar tropospheric ozone depletion events. *Atmos. Chem. Phys.* 9, 4639–4652. <https://doi.org/10.5194/acp-9-4639-2009>.
- Kalbitz, K., Kaiser, K., Bargholz, J., Dardenne, P., 2006. Lignin degradation controls the production of dissolved organic matter in decomposing foliar litter. *Eur. J. Soil Sci.* 57, 504–516. <https://doi.org/10.1111/j.1365-2389.2006.00797.x>.
- Kawamura, K., 1995. Land-derived lipid class compounds in the deep-sea sediments and marine aerosols from North Pacific. *Biogeochemical Processes and Ocean Flux in the Western Pacific*, pp. 31–51.
- Kawamura, K., Kasukabe, H., Barrie, L.A., 1996. Source and reaction pathways of dicarboxylic acids, ketoacids and dicarbonyls in arctic aerosols: one year of observations. *Atmos. Environ.* 30, 1709–1722. [https://doi.org/10.1016/1352-2310\(95\)00395-9](https://doi.org/10.1016/1352-2310(95)00395-9).
- Kellerman, A.M., Guillemette, F., Podgorski, D.C., Aiken, G.R., Butler, K.D., Spencer, R.G.M., 2018. Unifying concepts linking dissolved organic matter composition to persistence in aquatic ecosystems. *Environ. Sci. Technol.* 52, 2538–2548. <https://doi.org/10.1021/acs.est.7b05513>.
- Kim, S., Kramer, R.W., Hatcher, P.G., 2003. Graphical method for analysis of ultrahigh-resolution broadband mass spectra of natural organic matter, the Van Krevelen diagram. *Anal. Chem.* 75, 5336–5344. <https://doi.org/10.1021/ac034415p>.
- King, A.C.F., Thomas, E.R., Pedro, J.B., Markle, B., Potocki, M., Jackson, S.L., et al., 2019. Organic compounds in a sub-Antarctic ice Core: a potential suite of sea ice markers. *Geophys. Res. Lett.* 46, 9930–9939. <https://doi.org/10.1029/2019gl084249>.
- Koch, B.P., Dittmar, T., 2006. From mass to structure: an aromaticity index for high-resolution mass data of natural organic matter. *Rapid Commun. Mass Spectrom.* 20, 926–932. <https://doi.org/10.1002/rcm.2386>.
- Kopczynska, E.E., Dehaire, F., Elskens, M., Wright, S., 2001. Phytoplankton and microzooplankton variability between the subtropical and polar fronts south of Australia: thriving under regenerative and new production in late summer. *Journal of Geophysical Research: Oceans* 106, 31597–31609. <https://doi.org/10.1029/2000jc000278>.
- Kourchev, I., Fuller, S.J., Giorio, C., Healy, R.M., Wilson, E., O'Connor, L., et al., 2014. Molecular composition of biogenic secondary organic aerosols using ultrahigh-resolution mass spectrometry: comparing laboratory and field studies. *Atmos. Chem. Phys.* 14, 2155–2167. <https://doi.org/10.5194/acp-14-2155-2014>.
- Lieb-Lappen, R.M., Obbard, R.W., 2015. The role of blowing snow in the activation of bromine over first-year Antarctic Sea ice. *Atmos. Chem. Phys.* 15, 7537–7545. <https://doi.org/10.5194/acp-15-7537-2015>.
- Liu, J., Dedrick, J., Russell, L.M., Senum, G.I., Uin, J., Kuang, C., et al., 2018. High summertime aerosol organic functional group concentrations from marine and seabird sources at Ross Island, Antarctica, during AWARE. *Atmos. Chem. Phys.* 18, 8571–8587. <https://doi.org/10.5194/acp-18-8571-2018>.
- Longnecker, K., 2015. Dissolved organic matter in newly formed sea ice and surface seawater. *Geochim. Cosmochim. Acta* 171, 39–49. <https://doi.org/10.1016/j.gca.2015.08.014>.
- May, N.W., Quinn, P.K., McNamara, S.M., Pratt, K.A., 2016. Multiyear study of the dependence of sea salt aerosol on wind speed and sea ice conditions in the coastal Arctic. *J. Geophys. Res.-Atmos.* 121, 9208–9219. <https://doi.org/10.1002/2016jd025273>.
- Meyers-Schulte, K.J., Hedges, J.I., 1986. Molecular evidence for a terrestrial component of organic matter dissolved in ocean water. *Nature* 321, 61–63. <https://doi.org/10.1038/321061a0>.
- Mitra, S., Bianchi, T.S., Guo, L., Santschi, P.H., 2000. Terrestrially derived dissolved organic matter in the Chesapeake Bay and the middle Atlantic bight. *Geochim. Cosmochim. Acta* 64, 3547–3557.
- O'Dowd, C.D., De Leeuw, G., 2007. Marine aerosol production: a review of the current knowledge. *Philos. Trans. R. Soc. A Math. Phys. Eng. Sci.* 365, 1753–1774. <https://doi.org/10.1098/rsta.2007.2043>.
- O'Dowd, C.D., Facchini, M.C., Cavalli, F., Ceburnis, D., Mircea, M., Decesari, S., et al., 2004. Biogenically driven organic contribution to marine aerosol. *Nature* 431, 676.
- Ohkouchi, N., Kawamura, K., Kawahata, H., Taira, A., 1997. Latitudinal distributions of terrestrial biomarkers in the sediments from the Central Pacific. *Geochim. Cosmochim. Acta* 61, 1911–1918. [https://doi.org/10.1016/S0016-7037\(97\)00040-9](https://doi.org/10.1016/S0016-7037(97)00040-9).
- Opsahl, S., Benner, R., 1997. Distribution and cycling of terrigenous dissolved organic matter in the ocean. *Nature* 386, 480–482. <https://doi.org/10.1038/386480a0>.
- Park, J., Dall'Osto, M., Park, K., Kim, J.-H., Park, J., Park, K.-T., et al., 2019. Arctic primary aerosol production strongly influenced by riverine organic matter. *Environ. Sci. Technol.* 53, 8621–8630. <https://doi.org/10.1021/acs.est.9b03399>.
- Park, J., Jang, J., Yoon, Y.J., Kang, S., Kang, H., Park, K., et al., 2022. When river water meets seawater: insights into primary marine aerosol production. *Sci. Total Environ.* 807, 150866. <https://doi.org/10.1016/j.scitotenv.2021.150866>.
- Pautler, B.G., Simpson, A.J., Simpson, M.J., Tseng, L.-H., Spraul, M., Dubnick, A., et al., 2011. Detection and structural identification of dissolved organic matter in Antarctic glacial ice at natural abundance by SPR-W5-WATERGATE1H NMR spectroscopy. *Environ. Sci. Technol.* 45, 4710–4717. <https://doi.org/10.1021/es200697c>.
- Prather, K.A., Bertram, T.H., Grassian, V.H., Deane, G.B., Stokes, M.D., DeMott, P.J., et al., 2013. Bringing the ocean into the laboratory to probe the chemical complexity of sea spray aerosol. *Proc. Natl. Acad. Sci. U. S. A.* 110, 7550–7555. <https://doi.org/10.1073/pnas.1300262110>.
- Pusceddu, A., Cattaneo-Vietti, R., Albertelli, G., Fabiano, M., 1999. Origin, biochemical composition and vertical flux of particulate organic matter under the pack ice in Terra Nova Bay (Ross Sea, Antarctica) during late summer 1995. *Polar Biol.* 22, 124–132. <https://doi.org/10.1007/s003000050399>.
- Quinn, P.K., Bates, T.S., Schulz, K.S., Coffman, D., Frossard, A., Russell, L., et al., 2014. Contribution of sea surface carbon pool to organic matter enrichment in sea spray aerosol. *Nat. Geosci.* 7, 228. <https://doi.org/10.1038/ngeo2092>.
- Raphael, M.N., Handcock, M.S., 2022. A new record minimum for Antarctic Sea ice. *Nat. Rev. Earth Environ.* <https://doi.org/10.1038/s43017-022-00281-0>.
- Rhodes, R.H., Yang, X., Wolff, E.W., McConnell, J.R., Frey, M.M., 2017. Sea ice as a source of sea salt aerosol to Greenland ice cores: a model-based study. *Atmos. Chem. Phys.* 17, 9417–9433. <https://doi.org/10.5194/acp-17-9417-2017>.



- Rinaldi, M., Paglione, M., Decesari, S., Harrison, R.M., Beddows, D.C.S., Ovadnevaite, J., et al., 2020. Contribution of water-soluble organic matter from multiple marine geographic eco-regions to aerosols around Antarctica. *Environ. Sci. Technol.* 54, 7807–7817. <https://doi.org/10.1021/acs.est.0c00695>.
- Rontani, J.-F., Belt, S.T., Brown, T.A., Vaultier, F., Mundy, C.J., 2014. Sequential photo- and autoxidation of diatom lipids in Arctic Sea ice. *Org. Geochem.* 77, 59–71. <https://doi.org/10.1016/j.orggeochem.2014.09.009>.
- Russell, L.M., Hawkins, L.N., Frossard, A.A., Quinn, P.K., Bates, T.S., 2010. Carbohydrate-like composition of submicron atmospheric particles and their production from ocean bubble bursting. *Proceedings of the National Academy of Sciences* 107, 6652–6657.
- Safi Shalamzari, M., Ryabtsova, O., Kahnt, A., Vermeylen, R., Hérent, M.-F., Quetin-Leclercq, J., et al., 2013. Mass spectrometric characterization of organosulfates related to secondary organic aerosol from isoprene. *Rapid Commun. Mass Spectrom.* 27, 784–794. <https://doi.org/10.1002/rcm.6511>.
- Sarmiento, J.L., Quéré, C.L., 1996. Oceanic carbon dioxide uptake in a model of century-scale global warming. *Science* 274, 1346–1350. <https://doi.org/10.1126/science.274.5291.1346>.
- Schmale, J., Schneider, J., Nemitz, E., Tang, Y.S., Dragosits, U., Blackall, T.D., et al., 2013. Sub-Antarctic marine aerosol: dominant contributions from biogenic sources. *Atmos. Chem. Phys.* 13, 8669–8694. <https://doi.org/10.5194/acp-13-8669-2013>.
- Schmidt, F., Elvert, M., Koch, B.P., Witt, M., Hinrichs, K.-U., 2009. Molecular characterization of dissolved organic matter in pore water of continental shelf sediments. *Geochim. Cosmochim. Acta* 73, 3337–3358. <https://doi.org/10.1016/j.gca.2009.03.008>.
- Schmidt, F., Koch, B.P., Goldhammer, T., Elvert, M., Witt, M., Lin, Y.-S., et al., 2017. Unraveling signatures of biogeochemical processes and the depositional setting in the molecular composition of pore water DOM across different marine environments. *Geochim. Cosmochim. Acta* 207, 57–80. <https://doi.org/10.1016/j.gca.2017.03.005>.
- Schmitt-Kopplin, P., Liger-Belair, G., Koch, B.P., Flerus, R., Kattner, G., Harir, M., et al., 2012. Dissolved organic matter in sea spray: a transfer study from marine surface water to aerosols. *Biogeosciences* 9, 1571–1582. <https://doi.org/10.5194/bg-9-1571-2012>.
- Singer, G.A., Fasching, C., Wilhelm, L., Niggemann, J., Steier, P., Dittmar, T., et al., 2012. Biogeochemically diverse organic matter in alpine glaciers and its downstream fate. *Nat. Geosci.* 5, 710–714. <https://doi.org/10.1038/ngeo1581>.
- Stedmon, C.A., Markager, S., 2005. Tracing the production and degradation of autochthonous fractions of dissolved organic matter by fluorescence analysis. *Limnol. Oceanogr.* 50, 1415–1426. <https://doi.org/10.4319/lo.2005.50.5.1415>.
- Stubbins, A., Hood, E., Raymond, P.A., Aiken, G.R., Sleighter, R.L., Hernes, P.J., Butman, D., Hatcher, P.G., Striegl, R.G., Schuster, P., 2012. Anthropogenic aerosols as a source of ancient dissolved organic matter in glaciers. *Nat. Geosci.* 5 (3), 198. <https://doi.org/10.1038/Ngeo1403>.
- Wang, X., Deane, G.B., Moore, K.A., Ryder, O.S., Stokes, M.D., Beall, C.M., et al., 2017. The role of jet and film drops in controlling the mixing state of submicron sea spray aerosol particles. *Proc. Natl. Acad. Sci. U. S. A.* 114, 6978–6983. <https://doi.org/10.1073/pnas.1702420114>.
- Wang, Y., Yang, C., Li, J., Shen, S., 2014. The chemical composition and source identification of soil dissolved organic matter in riparian buffer zones from Chongming Island, China. *Chemosphere* 111, 505–512. <https://doi.org/10.1016/j.chemosphere.2014.04.056>.
- Wozniak, A.S., Bauer, J.E., Sleighter, R.L., Dickhut, R.M., Hatcher, P.G., 2008. Technical note: molecular characterization of aerosol-derived water soluble organic carbon using ultra-high resolution electrospray ionization fourier transform ion cyclotron resonance mass spectrometry. *Atmos. Chem. Phys.* 8 (17), 5099–5111. <https://doi.org/10.5194/acp-8-5099-2008>.
- Yang, X., Frey, M.M., Rhodes, R.H., Norris, S.J., Brooks, I.M., Anderson, P.S., et al., 2019. Sea salt aerosol production via sublimating wind-blown saline snow particles over sea ice: parameterizations and relevant microphysical mechanisms. *Atmos. Chem. Phys.* 19, 8407–8424. <https://doi.org/10.5194/acp-19-8407-2019>.
- Yang, X., Pyle, J.A., Cox, R.A., 2008. Sea salt aerosol production and bromine release: role of snow on sea ice. *Geophys. Res. Lett.* 35. <https://doi.org/10.1029/2008gl034536>.
- Zangrando, R., Corami, F., Barbaro, E., Grosso, A., Barbante, C., Turetta, C., et al., 2019. Free phenolic compounds in waters of the Ross Sea. *Sci. Total Environ.* 650, 2117–2128. <https://doi.org/10.1016/j.scitotenv.2018.09.360>.
- Zorn, S.R., Drewnick, F., Schott, M., Hoffmann, T., Borrmann, S., 2008. Characterization of the South Atlantic marine boundary layer aerosol using an aerodyne aerosol mass spectrometer. *Atmos. Chem. Phys.* 8, 4711–4728. <https://doi.org/10.5194/acp-8-4711-2008>.